Dynamics of Polymer Chains

Ulrike Genz

Max-Planck-Institut für Polymerforschung, Postfach 3148, D-55021 Mainz, FRG

Received December 30, 1993; Revised Manuscript Received May 25, 1994®

ABSTRACT: The generalized Rouse equation derived by Schweizer[1] is applied to chains in the crossover region between Rouse-like behavior and reptation-like behavior. A self-consistent scheme takes into account the coupling of single chain motion and the decay of density fluctuations in the polymer matrix. It will be shown that this model may be understood as a generalized bead–spring model, comprising beads with a frequency-dependent mobility and effective springs modified by their surroundings. The correlation functions of normal coordinates are investigated as a function of frequency, and strong qualitative deviations from the Rouse case with respect to the distribution of relaxation times are found. On this basis, general trends concerning viscoelasticity are elucidated and relevant time scales are discussed.

1. Introduction

The dynamics of individual polymer chains in a melt or in a concentrated polymer solution has been a topic of scientific interest for many years. A polymer melt behaves like a liquid when observed at longer times but also exhibits pronounced elastic features manifesting themselves in a plateau modulus in an intermediate frequency range.[2,3] What "long times" are in this context strongly depends on chain length. It is generally believed that these prominent features can—at least partly—be understood from the dynamical behavior of individual polymers. The study of self-diffusion, dielectric measurements,[4-6] and neutron scattering experiments[7,8] provided further knowledge on the chain dynamics, and various interpretations have been proposed.

The first microscopic approach to describe single chain motion was due to Rouse.[9] He modeled the polymer as a chain of statistical segments linked by entropic springs. Due to the viscous surroundings, these segments experience a frictional force described by a chain-length-independent segmental friction coefficient. Whereas this model is very successful in describing short chains, it fails for longer chains. Therefore, de Gennes[10] and Doi and Edwards[11] introduced the concept of reptation assuming that the lateral motion of a chain is strongly suppressed by its environment. This explained the appearance of a plateau modulus and the scaling of the self-diffusion coefficient with chain length. But the existence of a tube, or of entanglements, had to be postulated. To understand chain dynamics from a microscopic basis, Hess[12] applied projection operator techniques to derive an equation of motion for a single polymer. Keeping only those terms in the memory functions related to force autocorrelations, he arrived at a generalized Rouse equation identical in structure to an earlier heuristical proposal by Ronca,[13] but with the essential advantage that the memory function was expressed in terms of microscopic quantities. Schweizer[1,14,15] followed a similar approach and showed that correlations of forces due to the environment acting on neighboring segments also play an important role and may create typical polymer effects such as a plateau modulus.

This work is based on Schweizer's generalized Rouse equation.[1,14,15] Coupling between the collective motion of the matrix and the probe chain are taken into account explicitly while investigating the crossover region at intermediate chain lengths. Complementary to Schweizer's consideration in the time regime, the frequency dependence of several dynamical quantities is investigated.

This paper is organized as follows: Section 2 provides the generalized Rouse equation and describes approximations for the memory functions. In addition, numerical results for long-time self-diffusion and viscosity are shown. Sections 3 and 4 are aimed at an interpretation of the generalized Rouse equation. Section 5 elucidates the consequences on the relaxation of the correlation function of normal coordinates and discusses the effects on viscoelastic behavior. Various time scales arising from this description are discussed in section 6, and section 7 concludes.

2. Generalized Rouse Equation: Self-Diffusion and Viscosity

Schweizer[1,14,15] addressed the problem of understanding the motion of a probe chain interacting with other, identical chains on a microscopic basis. As a result of projection operator techniques, a mode–mode coupling approximation, and several simplifications applicable for Gaussian chains, he deduced a generalized Rouse equation describing the motion of a linear chain of N statistical segments. In addition to the entropic spring force of strength $K = 3k_BT/b^2$, where k_B is the Boltzmann constant, T the temperature, and b^2 the mean-squared distance of two neighboring segments, and a frictional force related to a segmental friction coefficient ξ independent of chain length N, memory terms account for the fact that the dynamics of the surrounding polymer matrix is not fast as compared to the single polymer motion. This generalized Rouse equation for the time development of the positions $\mathbf{r}_l(t)$ of the segments l of the probe chain also incorporates a stochastic force $\mathbf{f}_l(t)$ and is given by[1]

$$\xi\frac{d\mathbf{r}_l(t)}{dt} + \int_0^t d\tau\, \Xi(t-\tau)\frac{d\mathbf{r}_l(\tau)}{d\tau} - \int_0^t d\tau\, M(t-\tau)\frac{d}{d\tau}\frac{\partial^2}{\partial l^2}\mathbf{r}_l(\tau) = K\frac{\partial^2}{\partial l^2}\mathbf{r}_l(t) + \mathbf{f}_l(t) \quad (1)$$

in the overdamped limit. Equation 1 has been deduced for homopolymer chains and also applies to rings.[1] For block copolymers composed of different types of monomeric units or for star polymers, several steps in its derivation are not applicable. In the case of block copolymers it has been shown[16] that the equation of motion at a link between unlike blocks differs from eq 1 also with respect to its mathematical structure, whereas such an analysis has not been carried out for star polymers.

® Abstract published in *Advance ACS Abstracts*, September 1, 1994.

0024-9297/94/2227-6452$04.50/0

Therefore, such more complicated cases need a more profound investigation.

For linear homopolymers, the memory functions $\Xi(t)$ and $M(t)$ in eq 1 can be expressed as

$$\Xi(t) = \int \mathrm{d}k\, \mathcal{F}(k,t)\frac{1-f(k)}{1+f(k)} \tag{2}$$

and

$$M(t) = \int \mathrm{d}k\, \mathcal{F}(k,t)\frac{f(k)}{1-f^2(k)} \tag{3}$$

where

$$f(k) = \exp[-(kb)^2/6] = \exp[-(kR_G)^2/N] \tag{4}$$

$R_G = b(N/6)^{1/2}$ is the radius of gyration of the probe chain. The second factor in the integrand of eq 2 involving $f(k)$ scales as k^2 for small and intermediate k, whereas the corresponding factor in eq 3 scales as k^{-2} in this regime. For this reason, $\Xi(t)$, eq 2, is strongly influenced by the behavior of the integrand at $kR_G > 1$, whereas the small k region gives a major contribution to $M(t)$, eq 3.

The function $\mathcal{F}(k,t)$ is given by

$$\mathcal{F}(k,t) = \frac{k_B T}{2\pi^2}k^4N^2P^2(k)\, F_{self}(k,t)[\tilde{c}(k)]^2 I(k,t) \tag{5}$$

$P(k)$ is the Debye form factor of the Gaussian chain. $\tilde{c}(k)$ is the direct correlation function[17,18] and serves as a measure for the interactions between the probe polymer and the matrix. A quite common approximation is the replacement of the direct correlation function $\tilde{c}(k)$ by $-v$, where v is the excluded volume parameter. Besides neglecting additional density-dependent effects, such a procedure replaces the true, distance-dependent segmental interaction potential by $v\delta(\mathbf{r})$, where δ denotes the Dirac δ-function and $\mathbf{r}$ the segment separation. This may be sufficient on global length scales but cannot provide a proper description at short distances. Simply for mathematical reasons and to avoid the introduction of a cutoff $k_c \propto b^{-1}$ in the range of integration of eqs 2 and 3, the direct correlation function is approximated by

$$\tilde{c}(k) = -v \exp[-(kb)^2] \tag{6}$$

here. Because kb is quite small in the integration range of interest, this is only a minor correction.

$F_{self}(k,t)$ depends on the dynamics of the probe chain. In the spirit of a perturbation, it is approximated by its Rouse result,[11,14]

$$F_{self}(k,t) = \begin{cases} \exp[-k^2Dt] & \text{for } kR_G \ll 1 \\ \exp[-k^2(at)^{1/2}] & \text{for } kR_G \gg 1 \end{cases} \tag{7}$$

where

$$D = \frac{k_B T}{N\xi} \quad \text{and} \quad a = \frac{b^2 k_B T}{3\pi\xi} \tag{8}$$

In the numerical evaluation of the memory functions, the small k behavior is assumed to be valid up to $kR_G = \pi^{1/2}$, while for larger k the stretched exponential form is used. Schweizer, instead, employs the results of his renormalized Rouse model[14] to approximate $F_{self}(k,t)$. For long chains, this leads to a scaling behavior of various quantities in agreement with reptation theory. Because the renormalized Rouse model is essentially just a first approximation to include deviations from Rouse behavior, the theoretical justification to take these results as a starting point is not at all obvious. To avoid this still unsolved problem, chains in the crossover region deviating from Rouse-like behavior are considered within this perturbative ansatz.

The dynamic intensity characterizes the environment of the probe chain and is written as

$$I(k,t) = \frac{1}{V}\sum_{i,j}\langle \exp[i\mathbf{k}\cdot(\mathbf{r}_i^{(M)}(0) - \mathbf{r}_j^{(M)}(t))]\rangle \tag{9}$$

where the summation is performed over all segments i at positions $\mathbf{r}_i^{(M)}(t)$ of the polymer matrix. V is the volume of the system. Its static value $I(k) = I(k,t=0)$ is expressed in terms of the direct correlation function as[17,18]

$$I^{-1}(k) = \frac{1}{cNP(k)} - \tilde{c}(k) \tag{10}$$

which reduces to the random phase approximation (RPA)[10,19] when the direct correlation function $\tilde{c}(k)$ is replaced by $-v$. c denotes the number concentration of statistical segments. In a quite dense melt, large-scale concentration fluctuations determining $I(k\approx 0)$ are suppressed due to the presence of the second term in eq 10, $v = -\tilde{c}(0)$. In the limiting case of an incompressible melt, which is mathematically obtained by letting $v \to \infty$, $I(k)$ vanishes. However, the dependence of $\mathcal{F}(k,t=0)$, eq 5, on interaction strength and polymer concentration is determined by the factor $\tilde{c}^2(k)\, I(k)$, which, in the small k limit, may be cast in the form

$$\tilde{c}^2(0)\, I(0) = \frac{v}{b^3}\frac{vcN}{1+vcN}b^3 \tag{11}$$

when employing eqs 6 and 10. The first factor, v/b^3, is the ratio of the excluded volume v attributed to a segment to its geometrical size b^3 and has a finite value. The second factor reduces to unity in a melt of low compressibility or high v, whereas the remaining factor b^3 will be employed when substituting k by the dimensionless quantity kR_G in the integration. Therefore, the strong reduction of concentration fluctuations in a quite dense melt does not lead to a vanishingly low value of $\mathcal{F}(k,t)$, eq 5, or the memory functions.

Also some knowledge on the time dependence of $I(k,t)$ is necessary to determine $\mathcal{F}(k,t)$, eq 5. Important for low-frequency properties is its long-time behavior. Whereas simple short-time considerations predict a diffusive decay characterized by a diffusion coefficient $(k_B T/\xi)(c/I(k))$, which leads to a very fast rate due to the smallness of $I(k)$, typical dynamic light scattering experiments on melts show a nondiffusive decay of the dynamic scattering intensity. This finding has been explained as a coupling to longitudinal viscoelasticity.[20] In the similar case of concentrated polymer solutions, both a fast diffusive and a slow nondiffusive decay can be observed simultaneously.[21-23] The relative importance of fast and slow modes can be changed gradually while varying chain length, temperature, or polymer concentration. For the aim pursued here, it is far too complicated to distinguish between various time regimes, and, as a simplification, $I(k,t)$ is assumed to follow a single exponential decay characterized by the rate $\gamma_c(k)$,[1,24]

$$\gamma_c(k) = k^2\frac{k_B T}{\xi + k^2(\eta_\parallel/c)I(k)}\frac{c}{} \tag{12}$$

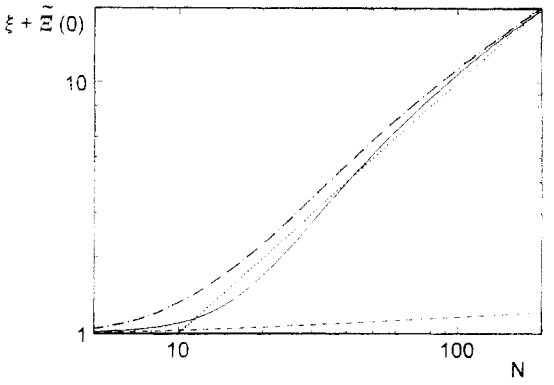

Figure 1. $(\xi + \tilde{\Xi}(0))$ in units of ξ as a function of N for $c\upsilon = cb^3 = 1$. The full line refers to the self-consistent treatment. Also included are the "mobile matrix" results $[\gamma_c = k^2(k_BT/\xi)(c/I(k))]$ (dashed line) and the "frozen matrix" results $[\gamma_c = 0]$ (dash–dotted line). The dotted line $\propto N$ indicates the reptation scaling prediction.

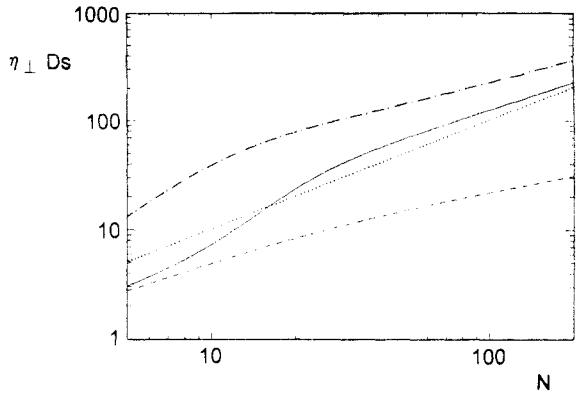

Figure 2. $\tilde{\eta}_\perp D_s/c$ in units of $(b^2k_BT/36)$ as a function of N for $c\upsilon = cb^3 = 1$. The full line refers to the self-consistent treatment. Also included are the "mobile matrix" results $[\gamma_c = k^2(k_BT/\xi)(c/I(k))]$ (dashed line) and the "frozen matrix" results $[\gamma_c = 0)$ (dash–dotted line). The dotted line $\propto N$ indicates the reptation scaling prediction.

where $\eta_\parallel$ is the longitudinal viscosity arising from the chain interactions. Obviously, this approximation is not well suited to treat very fast or high-frequency, processes and, as can be seen from the derivation of eq 12 in ref 24, is of limited applicability for larger values of k. When neglecting $\eta_\parallel$ in eq 12, γ_c reduces to the familiar short-time result, while the "frozen matrix" limit considered by Schweizer, $\gamma_c \to 0$, is approached for high viscosity. It will be shown in section 5 that an estimate on $\eta_\parallel$ consistent with eq 1 leads to

$$k^2\eta_\parallel/c \simeq \frac{(kR_G)^2}{3}[\xi + \tilde{\Xi}(0) + 6\tilde{M}(0)/N] \qquad (13)$$

where

$$\tilde{\Xi}(\omega) = \int_0^\infty dt\, \Xi(t) \exp[-i\omega t] \qquad (14)$$

is the one-sided Fourier transform of $\Xi(t)$, and $\tilde{M}(\omega)$ is defined correspondingly. Equations 12 and 13 allow for a self-consistent solution of $\tilde{\Xi}(0)$ and $\tilde{M}(0)$ in the following manner: An initial guess $\tilde{\Xi}_0(0)$ and $\tilde{M}_0(0)$ is made. From this guess, $\eta_\parallel$ is obtained by eq 13, which then gives the rate for the decay of the dynamic intensity, eq 12. This is employed to calculate the $\omega = 0$ values of the memory functions from eqs 2, 3, 5, and 14 and provides a new guess $\tilde{\Xi}_1(0)$ and $\tilde{M}_1(0)$. This procedure is iterated n times until the differences between $\tilde{\Xi}_n(0)$ and $\tilde{\Xi}_{n+1}(0)$ as well as $\tilde{M}_n(0)$ and $\tilde{M}_{n+1}(0)$ are negligible. Results depend on the chain length N, the reduced density of segments b^3c, and a measure for the interaction strength, $c\upsilon$. This scheme allows for the calculation of stationary transport coefficients and also forms the basis for the investigation of frequency-dependent quantities.

It has been shown[14] that the long-time self-diffusion coefficient of the chain obtained from eq 1 is given by

$$D_s = \frac{k_BT}{N(\xi + \tilde{\Xi}(0))} \qquad (15)$$

In the Rouse model, $\tilde{\Xi}(0)$ vanishes and D_s scales as N^{-1}. Reptation[10,11] leads to $D_s \propto N^{-2}$, which corresponds to a scaling $(\xi + \tilde{\Xi}(0)) \propto N$ within this treatment. Numerical results have been studied for a quite dense melt, $cb^3 = 1$, with strong interactions, $c\upsilon = 1$, and Figure 1 shows $(\xi + \tilde{\Xi}(0))$ as a function of chain length N. Starting from the Rouse result for very short chains, this quantity rises with increasing chain length for $N > N_c$. In the example given here, $N_c \simeq 10$ is obtained. For a lower polymer concentration, or a weaker interaction, a higher value of N_c results. For comparison, also the "mobile matrix" case neglecting $\eta_\parallel$ in eq 12 is shown. This simpler case does not show appreciable deviations from the Rouse result. Predictions from the "frozen matrix" approximation ($\gamma_c = 0$) are quite close to the self-consistent treatment for $(\xi + \tilde{\Xi}(0))$ or D_s. The scaling prediction of reptation theory is indicated as a straight line in Figure 1. This example illustrates the ability of the model to treat the crossover regime.

Internal relaxations are strongly influenced by $\tilde{M}(0)$. Within similar approximations as leading to eq 13, the product of shear viscosity $\tilde{\eta}_\perp$ and long-time self-diffusion coefficient can be written as

$$\tilde{\eta}_\perp(0)D_s/c \simeq \frac{b^2k_BT}{36}\left[1 + 6\frac{\tilde{M}(0)}{N[\xi + \tilde{\Xi}(0)]}\right] \qquad (16)$$

In the Rouse case, this product is independent of N. Also theories[12,13] starting from an equation similar to eq 1 with $M(t) = 0$ lead to $\tilde{\eta}_\perp D_s \propto O(N)$, while the original reptation model predicts $\tilde{\eta}_\perp(0)D_s \propto N$. Figure 2 shows the increase of this product with chain length. Also included in this figure are the "frozen matrix" and the "mobile matrix" results as well as the scaling prediction proportional to N. In contrast to the observations from Figure 1 related to self-diffusion, the discrepancies between the "frozen matrix" results and the self-consistent case are not negligible here and, therefore, the "frozen matrix" assumption may lead to an overestimation of internal relaxation times in this range of parameters.

The virtue of eq 1 is to provide a basis to study time- or frequency-dependent properties of a single chain, which will be discussed in the following.

3. Effective Segmental Friction and Mobility

This section elucidates the meaning of the memory function $\Xi(t)$. By partial integration, the corresponding term of eq 1 can be expressed in the form

$$\int_0^t dt'\, \Xi(t-t')\frac{d\mathbf{r}_l(t')}{dt'} = \Xi(t)[\mathbf{r}_l(t) - \mathbf{r}_l(0)] + \int_0^t dt' \left(\frac{d}{dt'}\Xi(t-t')\right)[\mathbf{r}_l(t) - \mathbf{r}_l(t')] \qquad (17)$$

Equation 17 contains a fading memory of a segment on its former positions. When considering self-diffusion in colloidal systems, a similar term arises and has been

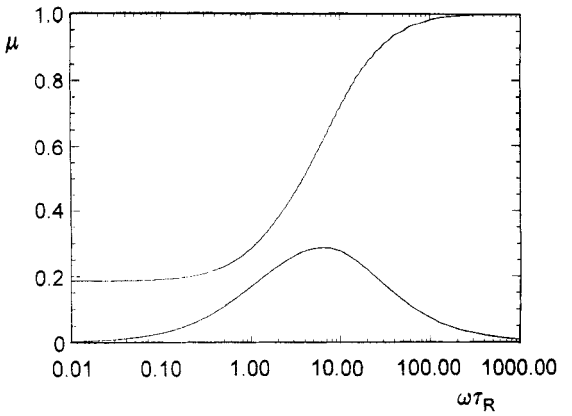

Figure 3. Real and imaginary parts of the mobility in units of $1/\xi$ as a function of $\omega\tau_R$. The parameters are $N = 50$ and $c\upsilon = cb^3 = 1$.

explained as a cage effect.[25] It causes non-Markovian behavior on intermediate time scales for the center-of-mass motion.

To provide an alternative interpretation, the motion of the probe chain in the presence of an external, oscillating force $\mathbf{F}_0 \exp[i\omega t]$ is considered. This force may simply be added to eq 1 when examining the linear response. By integrating over all segments, an equation for the center-of-mass is obtained, which is independent of $M(t)$. The mean velocity of the center-of-mass in the presence of the external force then also shows an oscillatory behavior,

$$\mathbf{v}(t) = \left\langle \frac{\mathrm{d}}{\mathrm{d}t}\frac{1}{N}\int_0^N \mathrm{d}l\, \mathbf{r}_l(t)\right\rangle_{\mathbf{F}_0} = \mathbf{v}_0 \exp[i\omega t] \qquad (18)$$

The complex amplitude

$$\mathbf{v}_0 = \frac{\mathbf{F}_0}{\xi + \tilde{\Xi}(\omega)} = \mu(\omega)\mathbf{F}_0 \qquad (19)$$

defines a frequency-dependent, complex mobility $\mu(\omega)$. In the limit $\omega \to 0$, it is directly related to the self-diffusion coefficient by $D_s = k_B T\mu(0)/N$; see eq 15.

This complex segmental mobility is calculated from eqs 14 and 19 within the approximations described in section 2, and a typical example is shown in Figure 3 for chains of length $N = 50$. At high frequencies, the real part of the segmental mobility coincides with the corresponding Rouse result $1/\xi$, whereas it decreases to $1/(\xi + \tilde{\Xi}(0))$ in the stationary case. At intermediate frequencies, the mobility also contains an imaginary component, indicating that velocity and force are out of phase. A qualitatively similar feature arises for the motion of a particle in a viscoelastic medium with complex viscosity. So the memory term involving $\Xi(t)$ essentially mimics the motion in an environment having viscoelastic, and not just viscous, properties.

From Figure 3, a typical time τ_μ characteristic for the crossover from a high mobility at short times to a low mobility for a stationary motion can be deduced. The dependence of this time on the chain length and its relation to other characteristic times is considered in section 6.

4. The Effective Spring

The second memory term related to $M(t)$ is a typical polymer effect and does not have an analogon in simple liquids or colloids. In the Markovian limit for long times, eq 1 may be written as

$$\left(\xi + \tilde{\Xi}(0) - \tilde{M}(0)\frac{\partial^2}{\partial l^2}\right)\frac{\mathrm{d}}{\mathrm{d}t}\mathbf{r}_l(t) = K\frac{\partial^2}{\partial l^2}\mathbf{r}_l(t) + \mathbf{f}_l(t) \qquad (20)$$

which formally corresponds to the generalization of the Rouse equation introduced by McInnes.[26] Here, a term analogous to a Cerf friction[10,27] results from a microscopic derivation.

The corresponding term in eq 1 can be written in analogy to eq 17 as

$$\int_0^t \mathrm{d}t'\, M(t-t')\frac{\partial^2}{\partial l^2}\frac{\mathrm{d}\mathbf{r}_l(t')}{\mathrm{d}t'} = M(t)\left[\frac{\partial^2}{\partial l^2}\mathbf{r}_l(t) - \frac{\partial^2}{\partial l^2}\mathbf{r}_l(0)\right] + \int_0^t \mathrm{d}t'\left(\frac{\mathrm{d}}{\mathrm{d}t'}M(t-t')\right)\left[\frac{\partial^2}{\partial l^2}\mathbf{r}_l(t) - \frac{\partial^2}{\partial l^2}\mathbf{r}_l(t')\right] \qquad (21)$$

As $(\partial^2\mathbf{r}_l/\partial l^2)$ describes local curvature and stretching of the chain, this term contains a fading memory of previous internal chain configurations. This is a qualitatively new feature in Schweizer's theory as compared to the results of Hess.[12]

Further insight is gained when considering the dynamics of normal coordinates,

$$\mathbf{R}_p(t) = \frac{1}{N}\int_0^N \mathrm{d}l \cos\left(\frac{p\pi l}{N}\right)\mathbf{r}_l(t), \qquad p = 1, 2, ..., N \qquad (22)$$

which diagonalize eq 1 and also the familiar Rouse equation. Their Fourier transforms,

$$\tilde{\mathbf{R}}_p(\omega) = \int_0^\infty \mathrm{d}t \exp[-i\omega t]\mathbf{R}_p(t) \qquad (23)$$

follow the equation of motion

$$\left[i\omega\mu^{-1}(\omega) + \left(\frac{\pi p}{N}\right)^2 K_{\mathrm{eff}}(\omega)\right]\tilde{\mathbf{R}}_p(\omega) = \left(\xi + \tilde{\Xi}(\omega) + \left(\frac{\pi p}{N}\right)^2 \tilde{M}(\omega)\right)\mathbf{R}_p(0) + \mathbf{f}_p \qquad (24)$$

where $\mathbf{f}_p$ is the stochastic force and the effective segmental mobility $\mu(\omega)$ has been defined in eq 19. The spring constant K of the familiar Rouse model is replaced by the quantity

$$K_{\mathrm{eff}}(\omega) = K + i\omega\tilde{M}(\omega) \qquad (25)$$

in the homogeneous part of eq 24. The imaginary part of $K_{\mathrm{eff}}(\omega)$ divided by ω has the meaning of an internal friction. Such an "effective spring" can be realized by coupling a spring with constant K to a dashpot–spring system. At higher frequencies, the restoring force is enhanced by this coupling, while the dashpot is not effective. At low frequencies, only the dashpot is important and the restoring force is entirely due to the bare spring constant K, while the friction is strongly enhanced. Of course, this has no effect on static properties. A typical frequency τ_K^{-1} can be obtained from the position of the maximum of the imaginary part of K_{eff}. The time τ_K is characteristic for a crossover from a dominantly elastic behavior to a strongly dissipative behavior and will be compared to other typical times in section 6.

5. Relaxations of Normal Modes

From the generalized Rouse equation (1), the time correlation function for the normal coordinates $\mathbf{R}_p(t)$, eq 22,

$$C_p(t) = \langle \mathbf{R}_p(t)\cdot\mathbf{R}_p(0)\rangle \qquad (26)$$

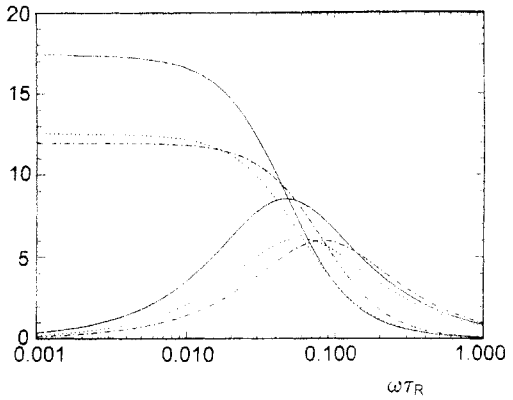

Figure 4. Correlation function of the normal coordinates, $\tilde{C}_p(\omega)/(C_p(0)\tau_R)$, for $p = 1$ (full line) and $p = 3$ (dotted line) as a function $\omega\tau_R$. Also shown is the Debye result characterized by the rate τ_G (- · -). The parameters are $N = 50$ and $c\upsilon = cb^3 = 1$.

can be studied by introducing their one-sided Fourier transforms $\tilde{C}_p(\omega)$. Equation 1 leads to

$$\frac{\tilde{C}_p(\omega)}{C_p(0)} = \left[\mathrm{i}\omega + \frac{1}{\tau(p,\omega)}\right]^{-1} \tag{27}$$

where

$$\tau(p,\omega) = \frac{\tau_R}{p^2}\left[1 + \frac{\tilde{\Xi}(\omega)}{\xi} + \left(\frac{\pi p}{N}\right)^2\frac{\tilde{M}(\omega)}{\xi}\right] \tag{28}$$

and

$$\tau_R = \frac{N^2b^2\xi}{3\pi^2k_BT} \tag{29}$$

is the Rouse time. The Rouse result is recovered from eqs 27 and 28 when neglecting the memory terms. Several essential differences to the Rouse case are evident: As $\tau(p,\omega)$ is a frequency-dependent quantity, the relaxation of $\tilde{C}_p(\omega)$ deviates from a Debye behavior, and, due to the increased friction, typical relaxation times can be much longer. In addition, the dependence on the mode index p differs strongly from the Rouse behavior due to the influence of $\tilde{M}(\omega)$. Two limiting cases can be distinguished: If the increase of the segmental friction discussed in section 3 is the dominant feature, the behavior at longer times is qualitatively similar to the Rouse result,

$$\tau(p,\omega\to 0) \simeq \frac{\tau_R}{p^2}\frac{\xi + \tilde{\Xi}(0)}{\xi} \tag{30}$$

If, instead, the internal friction of the effective spring discussed in section 4 gives the dominant influence, the relaxation at longer times is determined by

$$\tau(p,\omega\to 0) \simeq \frac{b^2\tilde{M}(0)}{3k_BT} = \tau_G \tag{31}$$

which is independent of the mode index p.

Figure 4 shows typical results for the real and imaginary parts of the dimensionless quantity $\tilde{C}_p(\omega)/(\tau_R C_p(0))$. The modes $p = 1$ and $p = 3$ are considered for a chain of length $N = 50$. Results for $p > 3$ are quite close to the curves obtained for $p = 3$. This shows that the term proportional to $\tilde{M}(\omega)$ in eq 28 dominates, and the effective segmental friction ($\xi + \tilde{\Xi}(\omega)$) is of minor importance for internal relaxations. Also indicated in Figure 4 is the Debye result, which is obtained when approximating $\tau(p,\omega)$ given in eq 28 by τ_G, eq 31. This simple approximation provides a reasonable guess for the order of magnitude and the typical frequencies for longer chains.

Figure 4 emphasizes on lower frequencies. Either directly from eq 1 reducing to the familiar Rouse equation in the short-time limit or when noting that $\tilde{\Xi}(\omega)$ and $\tilde{M}(\omega)$ both vanish in the high-frequency limit leading to $\tau(p,\omega\to\infty) \to \tau_R/p^2$ in eq 28, it is obvious that the similarity in decay times for the correlation functions of the normal coordinates related to different values of p only holds in such a low-frequency regime, whereas at high frequency the behavior approaches the Rouse result.

There is experimental evidence[28] that end blocks relax faster than blocks in the center of the chain. From the results presented here, conclusions on the motion of specific segments cannot be drawn straightforwardly, because the relation between normal coordinates and segment positions involves a transformation, eq 22, and because the displacement of a specific segment as a function of time is influenced by the behavior of normal coordinates at all frequencies. Generally speaking, low values of the mode index p refer to large-scale features of the time-dependent, accidental chain configuration, while higher values reflect distortions of the chain on smaller scales. According to the results discussed above, the latter can be as long-lived as the large-scale features, even if the initial relaxations at very short times are quite different. It will be shown later that this leads to a plateau behavior of the modulus, which cannot be reconciled with a Rouse-like distribution of relaxation times.

The frequency-dependent shear viscosity $\tilde{\eta}_\perp(\omega)$ is related to the corresponding time-dependent transport function by

$$\tilde{\eta}_\perp(\omega) = \int_0^\infty \mathrm{d}t\, \eta_\perp(t)\exp[-\mathrm{i}\omega t] \tag{32}$$

It is known from statistical mechanics[29] that $\eta_\perp(t)$ is determined by the time correlation function of the stress tensor. If forces along the chains give a dominant contribution to its xy component, $\eta_\perp(t)$ can be approximated by

$$\eta_\perp(t) = \frac{c}{Nk_BT}\sum_{lm}^{N}\langle F_{l,x}(0)\, y_l(0)\, F_{m,x}(t)\, y_m(t)\rangle \tag{33}$$

$F_{l,x}$ is the x-component of the force on segment l due to the entropic springs, and y_l is the y-component of the position of segment l. Equation 33 can be expressed in terms of normal coordinates, eq 22. This leads to a correlation function involving four normal coordinates, which is then factorized into a product of two correlation functions involving two normal coordinates each. As the normal coordinates for different mode indices, $p \neq p'$, are independent within this model, the result can be expressed in terms of the correlation functions $C_p(t)$, eq 26, as

$$\eta_\perp(t) = \frac{ck_BT}{N}\sum_{p=1}^{N}\left(\frac{C_p(t)}{C_p(0)}\right)^2 \tag{34}$$

which leads to the frequency-dependent modulus

$$\tilde{G}(\omega) = \mathrm{i}\omega\tilde{\eta}_\perp(\omega) = \mathrm{i}\omega\frac{ck_BT}{N}\sum_{p=1}^{N}\int_0^\infty \exp[\mathrm{i}\omega t]\left(\frac{C_p(t)}{C_p(0)}\right)^2 \tag{35}$$

So $\tilde{G}(\omega)$ depends on the behavior of $C_p(t)$ at all times, making it necessary to distinguish between different time or frequency regimes. Instead of performing an additional tedious numerical integration, it is more illustrative to show some consequences valid at lower frequencies. As has been shown above, the frequency dependence of $\tilde{C}_p(\omega)$ does not vary too strongly with mode index p for longer chains then, and a Debye behavior with the time τ_G, eq 31, provides an estimate for the typical times. Within this simplifying assumption, the real part of the modulus,

$$G'(\omega) \simeq ck_BT\frac{\omega^2}{\omega^2 + (2/\tau_G)^2} \tag{36}$$

has a Debye form. For small ω, it vanishes as ω^2, which is typical for a fluid. For $\omega > 2/\tau_G$, a plateau regime is expected. The height of this plateau is independent of chain length and is approximately given by ck_BT. This estimate is higher than the value ck_BT/N_e expected for polymer melts, where N_e gives the number of segments between entanglements and is commonly introduced as an additional parameter. The overestimation may partly be due to the crude approximation of $C_p(t)$ by a single exponential function characterized by the slow, long-time-limiting decay rate. The appearance of a plateau modulus with a height independent of chain length is typical for polymeric systems[2,3] and is commonly attributed to the existence of entanglements. Here, these tendencies result from the presence of $\tilde{M}(\omega)$.

The stationary viscosity $\tilde{\eta}_\perp(0)$ can be calculated within the same approximation, and the relation

$$\tilde{\eta}_\perp(0) \simeq ck_BT\tau_G/2 \tag{37}$$

is obtained. A proportionality of viscosity and typical viscoelastic time has also been observed experimentally.[2,3]

The calculation of $\tilde{\eta}_\perp(0)$ and $\eta_\parallel$ in section 2 is also based on eq 34 and a corresponding expression for the longitudinal viscosity. To obtain eqs 13 and 16, typical times for the decay of $C_p(t)$ have been obtained from $\tau(p,0)$ as given in eq 28, and not from the approximative result in eq 31.

The results of this section suggest a strong slowing down of all internal relaxations for longer chains. The relaxation for the end-to-end vector of specific blocks, or subunits, on a chain is thus expected to be strongly influenced by the total chain length and much slower than expected from a Rouse-like behavior. For block copolymers, a strong increase of the relaxation times of blocks as compared to the Rouse result is confirmed experimentally,[30,31] but the interpretation of such experiments is not straightforward as the blocks differ in their microscopic frictional properties and composition fluctuations, which are not included here, also play a role.

6. Typical Times

Having an overview on various dynamical processes related to the single chain motion, the typical times depending on chain length are investigated. The results are summarized in Figure 5, and it is the aim of this section to explain these data.

In section 3, an effective segmental mobility $\mu(\omega)$ was introduced by eq 19. The time τ_μ determined from the position of the maximum of its imaginary part is characteristic for the crossover from a high mobility $1/\xi$ at short times to a low mobility $1/(\xi + \tilde{\Xi}(0))$ at long times. Assuming $cv = cb^3 = 1$, numerical values for this time are given in Figure 5 as a function of chain length N. It can

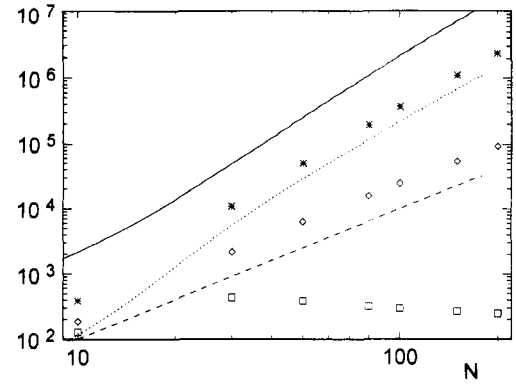

Figure 5. Typical times in units of $b^2\xi/(3\pi^2k_BT)$ as a function of chain length N. Rouse time τ_R is indicated by the dashed line, τ_G refers to the dotted line, and the full line indicates τ_s. Symbols refer to τ_μ (□), τ_K (◇), and τ_E (*).

be seen that τ_μ hardly depends on chain length and is quite short as compared to all other times included in this figure. An independence of chain length supports the interpretation of the related process as a caging effect, which is a local feature. For times longer than τ_μ, the segment mobility is already strongly reduced due to the presence of the surrounding matrix. At $t = \tau_\mu$, a specific mean-squared displacement a^2 of a segment is expected. The dependence of the mobility on frequency then leads to the following effect: For a displacement smaller than a, the segments appear to be quite mobile, whereas for larger displacements, the mobility is strongly reduced. This may qualitatively explain the experimental observation[7,8] of a time/length scale typical for the deviation from Rouse behavior, which has been interpreted as an indication for a "tube", in which segments may move quite freely. Within this model, such a time scale may also be present for short chains, but the effect on the mobility is negligible then.

In section 4, it has been illustrated that a second type of memory effect due to $M(t)$ can be interpreted as a modification of the entropic spring. At short times, the elastic character of the surrounding polymer matrix leads to an enhancement of the restoring forces, while at long times a considerable additional friction arises. The maximum of the imaginary part of K_{eff} at $\omega_K = 1/\tau_K$ is typical for the frequency at which the effective spring loses its dominantly elastic character and exhibits strongly dissipative features. Numerical results in Figure 5 show that τ_K increases with chain length similar to the Rouse time τ_R also included in Figure 5.

As has been noted in section 5, the crossover frequency for the plateau modulus is expected at a typical time τ_G, eq 31. This time included in Figure 5 increases less steeply than N^3 in these examples. For longer chains, such a time is expected to scale as the viscosity, which experimentally was found to increase as $N^{3.4}$. The original form of reptation theory predicts an increase as N^3, while a more refined numerical study by O'Connor and Ball[32] on the Doi–Edwards model found a $N^{3.4}$ dependence, in agreement with experiment.

Typical times τ_E of the relaxation of the end-to-end vector, $\mathbf{R}_E(t)$, are obtained from the Fourier transform of

$$\langle \mathbf{R}_E(t)\cdot\mathbf{R}_E(0)\rangle = 16\sum_{p\ \mathrm{odd}} C_p(t) \tag{38}$$

These times are also included in Figure 5 and are found to be somewhat longer than τ_G, because they are strongly determined by the contribution from $p = 1$, having the slowest decay of all internal relaxations. For longer chains, a similarity between times for the normal mode process

and the time characterizing the onset of the plateau regime in the modulus is implied. Experimentally,[5,6] a scaling of $\tau_E \propto N^{3.7}$ has been reported.

A typical time for self-diffusion of the chain is

$$\tau_s = \frac{(2R_G)^2}{D_s} = \frac{2b^2\xi}{3k_BT}N^2\frac{\xi + \tilde{\Xi}(0)}{\xi} \qquad (39)$$

It is the longest time included in Figure 5. For a quite flexible chain, self-diffusion of the entire chain over a distance comparable to its size is generally expected to be the slowest process.

Concerning the various times, it is useful to remember some quite general arguments. When assuming $D_s \propto N^{-2}$ and $R_G \propto N$, which is commonly expected for longer chains, the time τ_s in eq 39 rises with chain length as N^3. If the longest internal relaxation time is assumed to scale as $N^{3.4}$ even in an asymptotic long chain regime, it becomes larger than τ_s beyond a certain chain length. This would imply that the chain has moved a distance comparable to its size without completely changing its internal configuration and contradicts common expectations on the motion of a highly flexible chain. This illustrates the importance of investigating several dynamical properties simultaneously when modeling or describing single chain behavior.

The data presented in Figure 5 have been calculated within the approximations in section 2 aimed at a study of chains in a crossover range. Therefore, asymptotic scaling laws cannot be derived from here. But it is evident that results of this quite detailed model are in keeping with general expectations.

7. Conclusions

The generalized Rouse equation derived by Schweizer[1,14] has been investigated with emphasis on the frequency dependence of various quantities. Memory functions contain the influence of the surrounding polymer matrix on the probe polymer. Therefore, it is important to model dynamical features of the surroundings sufficiently well. A self-consistent treatment of collective and single chain dynamics showing substantial deviations from simpler schemes has been developed. This part of the work may be useful for future investigations improving on the modeling of the memory functions.

A second topic of this work concerns the interpretation of the generalized Rouse equation. A picture of an effective bead–spring system is suggested, which may be helpful for a more intuitive understanding. Because of the presence of two kinds of memory functions, several time scales appear naturally, depending on chain length in different ways. Further investigations, as the influence on interaction strength and segment density, may be performed along similar lines to provide a more complete description.

The various numerical examples addressed the case of chains in a crossover region where a perturbative treatment based on the Rouse result is meaningful. However, the general framework of this description, including the relevance of various typical time scales, the mathematical description of the relaxation of the correlation functions of normal coordinates, and the interpretation proposed for the memory functions, can also be applied to long chains, and the ideas presented here may provide additional guidelines and impulses on the interpretation of various experimental results.

Acknowledgment. This work has been supported by the Deutsche Forschungsgemeinschaft, SFB 262.

References and Notes

(1) Schweizer, K. S. *J. Chem. Phys.* **1989**, *91*, 5822.
(2) Ferry, J. D. *Viscoelastic Properties of Polymers*; John Wiley & Sons: New York, 1980.
(3) Pearson, D. S. *Rubber Chem. Technol.* **1987**, *60*, 439.
(4) Bauer, M. E.; Stockmayer, W. H. *J. Chem. Phys.* **1965**, *43*, 4319.
(5) Adachi, K.; Kotaka, T. *Macromolecules* **1984**, *17*, 120; **1985**, *18*, 466.
(6) Boese, D.; Kremer, F. *Macromolecules* **1990**, *23*, 829.
(7) Higgins, J. S.; Roots, J. E. *J. Chem. Soc., Faraday Trans. 2* **1985**, 757.
(8) Richter, D.; Farago, B.; Fetters, L. J.; Huang, J. S.; Ewen, B.; Lartigue, C. *Phys. Rev. Lett.* **1990**, *64*, 1389. Richter, D.; Butera, R.; Fetters, L. J.; Huang, J. S.; Farago, B.; Ewen, B. *Macromolecules* **1992**, *25*, 6156. Richter, D.; Farago, B.; Butera, R.; Fetters, L. J.; Huang, J. S.; Ewen, B. *Macromolecules* **1993**, *26*, 795.
(9) Rouse, P. E. *J. Chem. Phys.* **1953**, *21*, 1272.
(10) De Gennes, P.-G. *Scaling Concepts in Polymer Physics*; Cornell University Press: Ithaca, NY, 1979.
(11) Doi, M.; Edwards, S. F. *The Theory of Polymer Dynamics*; Clarendon Press: Oxford, 1986.
(12) Hess, W. *Macromolecules* **1988**, *21*, 2620.
(13) Ronca, G. *J. Chem. Phys.* **1983**, *79*, 1031.
(14) Schweizer, K. S. *J. Chem. Phys.* **1989**, *91*, 5802.
(15) Schweizer, K. S. *J. Non-Crystall. Solids* **1991**, *131*, 643; *Phys. Scr.* **1993**, *T49*, 99.
(16) Genz, U.; Vilgis, T. A. Dynamics of Block Copolymer Chains Near the Microphase Separation Transition. *J. Chem. Phys.* **1994**, in press.
(17) Schweizer, K. S.; Curro, J. G. *Phys. Rev. Lett.* **1987**, *58*, 246. Curro, J. G.; Schweizer, K. S. *Macromolecules* **1987**, *20*, 1928. Schweizer, K. S.; Curro, J. G. *J. Chem. Phys.* **1988**, *89*, 3342. Yethiraj, A.; Schweizer, K. S. *J. Chem. Phys.* **1992**, *97*, 1455.
(18) Genz, U.; Klein, R. *J. Phys. Fr.* **1989**, *50*, 439.
(19) Vilgis, T. A.; Benmouna, M.; Benoit, H. *Macromolecules* **1991**, *24*, 4481.
(20) Wang, C. H.; Fischer, E. W. *J. Chem. Phys.* **1985**, *82*, 632. Wang, C. H.; Fytas, G.; Fischer, E. W. *J. Chem. Phys.* **1985**, *82*, 4332.
(21) Nicolai, T.; Brown, W.; Hvidt, S.; Heller, K. *Macromolecules* **1990**, *23*, 5088.
(22) Brown, W.; Johnsen, R. M.; Konak, C.; Dvoranek, L. *J. Chem. Phys.* **1991**, *95*, 8568.
(23) Koch, T.; Strobl, G.; Stühn, B. *Macromolecules* **1992**, *25*, 6255.
(24) Genz, U. Collective Diffusion in Polymer Solutions. *Macromolecules* **1994**, *27*, 3501.
(25) Pusey, P. N. *J. Phys. A: Math. Gen.* **1978**, *11*, 119.
(26) McInnes, D. A.; North, A. M. *Polymer* **1977**, *18*, 505.
(27) Cerf, R. *J. Phys. Radium* **1958**, *19*, 122.
(28) Tassin, J. F.; Monnerie, L.; Fetters, L. J. *Macromolecules* **1988**, *21*, 2404.
(29) Boon, J. P.; Yip, S. *Molecular Hydrodynamics*; McGraw-Hill: New York, 1980.
(30) Adachi, K.; Nishi, I.; Doi, H.; Kotaka, T. *Macromolecules* **1991**, *24*, 5843.
(31) Alig, I.; Kremer, F.; Fytas, G.; Roovers, J. *Macromolecules* **1992**, *25*, 5277.
(32) O'Connor, N. P. T.; Ball, R. C. *Macromolecules* **1992**, *25*, 5677.